Phase Separation Morphology of Thin Films of Polystyrene/ Polyisoprene Blends

K. DALNOKI-VERESS, J. A. FORREST, J. R. STEVENS, and J. R. DUTCHER*

Department of Physics and The Guelph-Waterloo Program for Graduate Work in Physics, University of Guelph, Guelph, Ontario, Canada N1G 2W1

SYNOPSIS

We present the results of a study of the morphology of phase separation in a thin film blend of polystyrene (PS) and polyisoprene (PI) in a common solvent of toluene. The blend is quenched by rapid solvent evaporation using a spincoating technique rather than a temperature quench. The mass fraction of polystyrene is varied to determine the effect of the substrate on thin film phase separation morphology. We compare the phase separation morphology for very thin films of the PS/PI blend cast onto three different substrates: Si(001) with a native oxide layer (Si–SiO_x), Si(001) etched in hydrofluoric acid (Si–H), and a Au/Pd alloy sputtered onto Si(001). We observe large differences between the morphologies of 1000 Å thick blend films on the Si–SiO_x and Si–H substrates as the mass fraction is varied due to the difference in the wetting properties of PS on the two substrates. Smaller differences are observed between the films on the Si–SiO_x and Au/Pd substrates only for film thicknesses $h < 600$ Å.
Keywords: phase separation morphology • thin films

INTRODUCTION

The effect of a surface on phase separation of thin film blends is of great interest both experimentally and theoretically,[1-9] and clearly becomes important as the surface-to-volume ratio is increased. In this article we focus on the effect of the substrate on the morphology of phase-separated thin film blends that are quenched into the unstable part of the phase diagram.

Typically, a quench of the polymer blend is achieved by a rapid change of temperature which forces the blend into the unstable or metastable regions of the phase diagram. In the metastable region of the phase diagram, between the binodal and spinodal lines, phase separation takes place by nucleation and growth.[10] Phase separation in the unstable region occurs via spinodal decomposition bounded by the spinodal line.[10,11] The morphology of the phase-separated domains can be used to understand the mechanisms of phase separation. It has been shown both by simulation[1,12,13] and experiment[14-16] that generally a bicontinuous morphology results from a critical quench for which the blend composition is that corresponding to the critical composition, and a droplet-like morphology is obtained for an off-critical quench.

The bicontinuous morphology is not always obtained for blends of the critical composition. A dramatic example of this occurs for polymer blend thin films for which the individual polymer components segregate to the free film surface and the film–substrate interface. This leads to a bilayer structure if one component prefers the substrate and the other component prefers the free surface, or a trilayer structure if one component prefers both the substrate and the free surface.[2,3,5] Substantial surface roughnening resulting from phase separation within the film plane has also been observed for annealed spincoated polymer blend films.[17] The bicontinuous morphology may also occur for a mass fraction which is shifted from the critical mass fraction due to large differences in the dynamic properties of the two polymer components.[8,18] The effect of shear on phase separation, which leads to an anisotropic morphology, has also been studied.[19]

* To whom correspondence should be addressed.

Journal of Polymer Science: Part B: Polymer Physics, Vol. 34, 3017–3024 (1996)
 CCC 0887-6266/96/173017-08

Usually phase separation in complex fluids is studied for the case of a two-polymer melt. However, this may be problematic if the two components have substantially different glass transition temperatures (T_g), since the lower T_g component may degrade for temperatures greater than the T_g value for the other component. One way to study a system with large differences in the glass transition temperatures of the polymer components is to use a three-component or ternary system: two polymers in a common solvent. For a solvent quench, in which the solvent is removed rapidly from the solution, phase separation of the two polymer components can be observed.

In the present article we discuss the effect of three different substrates on the morphology of phase separation in thin films of polystyrene/polyisoprene blends quenched by solvent evaporation. Since PS and PI have glass transition temperatures of 100°C and −70°C, respectively, it is difficult to study this system as a binary blend because the PI degrades at temperatures greater than the PS glass transition temperature. This polymer blend is a good choice for study as a ternary system since rapid evaporation of toluene is possible using spincoating. The average area of the domains of one polymer component within a matrix of the other polymer component is used as a quantitative measure of the observed morphologies. We observe differences in the morphologies for the different substrates that are due to differences in the wetting properties of the two polymers on the substrates. We also identify some aspects of the ternary phase diagram.

EXPERIMENTAL

Materials and Sample Preparation

The ternary solutions consisted of polystyrene (PS) and polyisoprene (PI) dissolved in toluene, which is a good solvent for both polymer components. The polymers[20] had molecular weights $\bar{M}_w$ = 760,000 (PS) and $\bar{M}_w$ = 410,000 (PI) and polydispersities $\bar{M}_w/\bar{M}_n$ = 1.10 (PS) and $\bar{M}_w/\bar{M}_n$ = 1.06 (PI). For the ternary solutions, the total polymer concentration was fixed at 2.00% and the PS mass fraction (ϕ_m) was varied between 0 and 1. Thin films of the polymer blends were formed by placing a droplet of the solution onto a 1 cm × 1 cm substrate spinning at 3000 rpm. This combination of total polymer concentration and spin speed resulted in films with thickness $h \sim 1000$ Å.

The films were deposited at room temperature onto three different substrate types: (1) Si(001) with the native oxide layer present (Si–SiO_x); (2) hydrogen-terminated Si(001) (Si–H); and (3) a 200 Å thick 60% Au/40% Pd (Au/Pd) layer sputtered onto Si(001). The Si–H surface was made by dipping the Si(001) wafer into a 20% hydrogen fluoride (HF) solution for 10 s. The HF solution removes the native oxide layer and leaves a hydrogen-terminated substrate.[21,22] To avoid the possible reoxidation[22] of the substrate, spincoating was done immediately after the HF dip followed by a rinse with deionized water. Because the PS and PI on the three substrate types have different wetting properties it was expected that there would be differences between the morphologies of the phase-separated domains for the different substrate types. We found that the PS molecules used in this study dewet on Si–SiO_x after annealing the films for 24 h in a vacuum oven at a temperature of 160°C (which is 60°C above the PS glass transition temperature). In contrast, the PS molecules on the other two substrates showed no dewetting after 1 week under the same conditions. In a period of 1 week the PI molecules used in this study do not dewet on any of the substrate types at room temperature, which is 90°C above the PI glass transition temperature.

Data Analysis

The morphology of the phase-separated thin films was measured at room temperature using a metallurgical optical microscope. A CCD camera was adapted to the microscope and interfaced through a PC-based frame grabber to obtain digital images. Since the characteristic length of most of the domains is larger than 3 μm, optical microscopy was sufficient to measure the phase-separated domain areas. It was not necessary to use stains to enhance the optical contrast; the difference in index of refraction for PS and PI ($\Delta n \sim 0.07$) is sufficient to ensure that the colors of the two phases were different for films with thickness $h \sim 1000$ Å. Different colored optical filters were also used with the microscope to enhance the contrast. This method of digital image acquisition allowed us to measure the morphologies for all of the 1000 Å thick films. However, for the measurement of very thin films ($h \sim 350$ Å), the optical contrast is low and the resulting image quality is poor.

Care was taken to obtain images of the morphology only near the center of the spincoated films so that the effect of shear on phase separation[19] is not an important factor. This is a precaution (not a necessity) for the PS/PI blend thin films since little difference was observed between the mor-

phologies near the center and the outer edge of the film where shear effects should be the largest. The different PS-rich and PI-rich phases in the film were identified by selectively dissolving away the PI with heptane so that only the PS-rich phase remained.

As a quantitative measure of the film morphology, we chose to measure the area of the domains present in the digital images. The domain areas were measured for different values of the PS mass fraction ϕ_m on the three substrates using commercial image analysis software. For each ϕ_m value we required that a minimum of 150 domains be used in the analysis; multiple images were used if necessary to ensure that the results were statistically significant. It was necessary to relax this requirement for $\phi_m = \phi_{m,b}$, corresponding to the bicontinuous morphology, for which the domain areas are very large and the number of domains was therefore very small. Domain area measurements were performed rather than measurements of the domain perimeters because perimeter measurements were shown to have greater error in digital images.

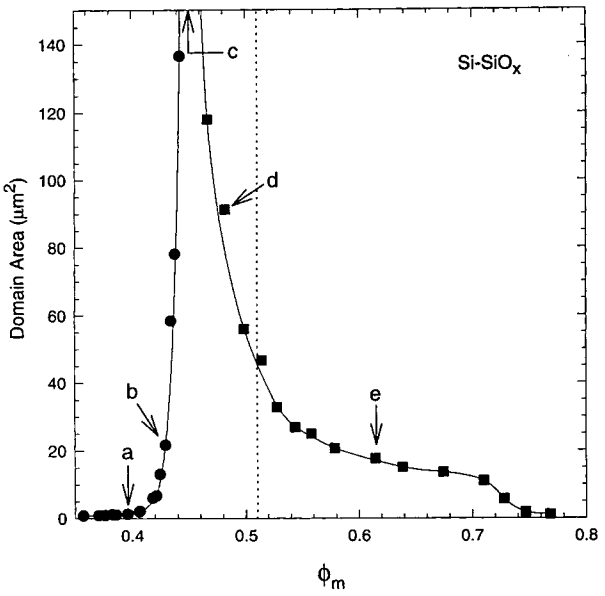

Figure 1. Average domain area versus PS mass fraction ϕ_m for 1000 Å thick PS/PI blend films on Si–SiO_x substrates. The curves are intended to guide the eye. The letters identify data points corresponding to the morphology images shown in Figure 2. The vertical dashed line corresponds to $\phi_m = \phi_{m,c}$.

RESULTS AND DISCUSSION

We begin by discussing some of the general aspects of the morphologies observed for the thin film PS/PI system. The phase-separated domains were flat, as evidenced by their uniform color, with typically a single optical fringe observed near the domain boundaries. The curvature of the surface was small since the domain diameter was generally a factor of 50 larger than the film thickness.

Typical results for the Si–SiO_x substrate are shown in Figure 1 as a plot of the average domain area versus PS mass fraction ϕ_m. Five points are labeled which correspond to the digital images of the observed morphologies shown in Figure 2. It may be seen from Figure 1 that small PS-rich domains are present in a PI-rich matrix for small values of ϕ_m. As ϕ_m is increased, the domains increase in size until a bicontinuous morphology is obtained for $\phi_m = \phi_{m,b} = 0.45 \pm 0.02$. We note the extremely narrow range over which the bicontinuous morphology can be observed. The critical mass fraction $\phi_{m,c}$ can be calculated using the Flory–Huggins theory for binary polymer blends.[23] For the polymer molecules used in this study, $\phi_{m,c} = 0.51$. There is a substantial difference between $\phi_{m,c} = 0.51$ and the PS mass fraction for which the bicontinuous morphology is observed; this difference is currently being investigated. As ϕ_m is increased further, the interconnected PI-rich domain breaks up and smaller PI-rich domains are formed in a PS-rich matrix.

The measured average domain area for each substrate type is shown as a function of ϕ_m in Figure 3. There is a very large difference between the results for the Si–H and Si–SiO_x substrates. For the Si–H substrate there is a transition from domains of one component to domains of the other component over a much larger range of ϕ_m values than for the Si–SiO_x substrate. For the Si–H substrate, reliable domain area measurements were not possible for $0.5 \lesssim \phi_m \lesssim 0.7$, since complex, three-dimensional morphologies were observed. For $\phi_m < 0.5$ and $\phi_m > 0.7$ the morphologies for the Si–H substrate were qualitatively similar to those observed for PI-rich and PS-rich domains on the Si–SiO_x substrate.

If we compare the morphologies obtained for different values of ϕ_m for the Si–SiO_x substrate shown in Figure 2, we see that all of the PS-rich domains formed for $\phi_m = 0.40$ are circular, whereas many of the PI-rich domains for $\phi_m = 0.61$ are elongated. It is possible that the difference in domain shapes for these two values of ϕ_m is due to the difference in the interaction of the two polymers with the substrate, since PI in the melt phase wets the Si–SiO_x substrate in contrast to PS which dewets upon annealing. This means that the formation of circular domains from elongated domains is more energetically favorable

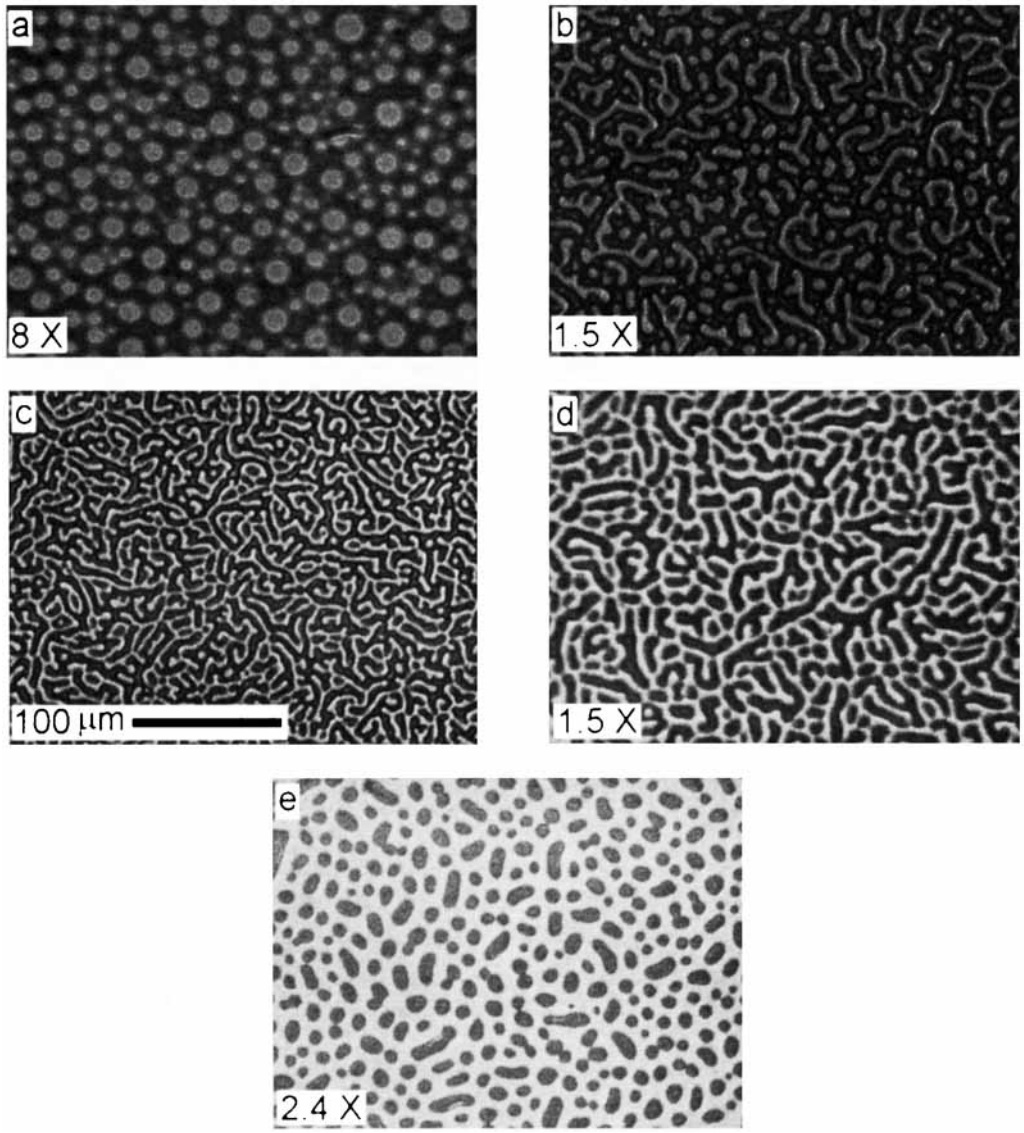

Figure 2. Morphology images for 1000 Å thick PS/PI blend films on Si–SiO_x substrates. The images correspond to the data points identified in Figure 1. The ϕ_m values are (a) 0.40, (b) 0.43, (c) 0.45, (d) 0.48, and (e) 0.61.

for PS than for PI, which would make the observation of circular domains for small values of ϕ_m more likely than for large values of ϕ_m. However, this effect is overwhelmed by the influence of the polymer/air interactions (surface tensions). Since the PS surface tension γ_{PS} = 40 dyn/cm is larger than the PI surface tension γ_{PI} = 32 dyn/cm, PS-rich domains obtained for small values of ϕ_m will tend to be more circular than PI-rich domains obtained for large values of ϕ_m. Therefore, the difference in surface tensions can also explain the difference in the domain shapes observed for the Si–SiO_x substrate for ϕ_m = 0.40 and ϕ_m = 0.61. The surface tensions must dominate the phase separation morphologies because the morphologies measured for the Au/Pd substrate are indistinguishable from those observed for the Si–SiO_x substrate, even though PS wets the Au/Pd substrate much more readily than the Si–SiO_x substrate, as shown by the dewetting studies described above. The striking similarity of the morphologies for the Si–SiO_x and Au/Pd substrates, as can be seen clearly by comparing the dependence of the average domain area on ϕ_m in parts (b) and (c) of Figure 3, means that the effect of the polymer/substrate interactions must be small compared with the effect of the surface

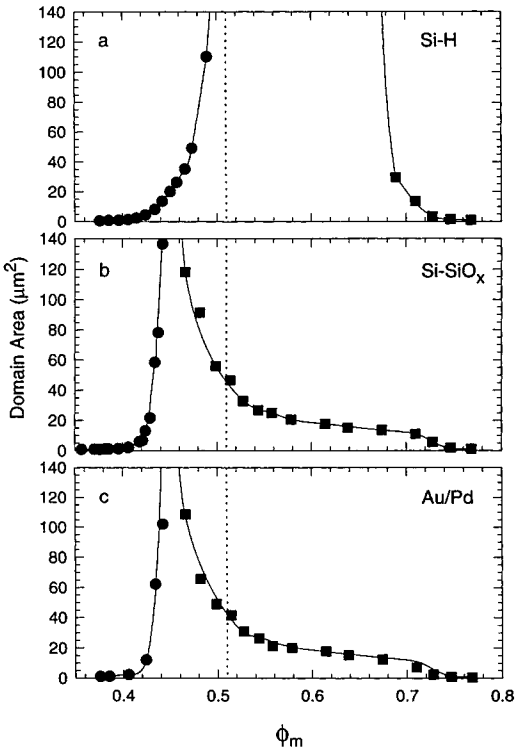

Figure 3. Average domain area versus PS mass fraction ϕ_m for 1000 Å thick PS/PI blend films on different substrates. The curves are intended to guide the eye. The vertical dashed lines correspond to $\phi_m = \phi_{m,c}$.

tensions for 1000 Å thick films on the Si–SiO_x and Au/Pd substrates. In contrast, the large difference in morphologies obtained for the Si–SiO_x and Si–H substrates discussed above suggests that the large difference in the wetting properties of PS on the two substrates is responsible for the large differences in the morphologies observed for the 1000 Å thick films.

The striking similarity of the morphologies observed for 1000 Å thick films on the Si–SiO_x and Au/Pd substrates leads one to the following question: how small does the film thickness have to be to observe differences in morphology between films on the Si–SiO_x and Au/Pd substrates?

To address this question, we reduced the PS/PI blend film thickness by reducing the total polymer concentration from 2.00% to 0.77%. For a spin speed of 3000 rpm, this reduces h from 1000 to 350 Å. Because the average domain area is very sensitive to small changes in ϕ_m near $\phi_{m,b}$ we fixed $\phi_m = 0.45$ to observe shifts in the morphology due the substrate. The resulting morphologies for the Si–SiO_x and Au/Pd substrates are shown in Figure 4 together with the morphology observed for a 1000 Å thick film. It is worth noting that the bicontinuous morphology of Figure 4 is virtually identical to that observed in Figure 2. These two photographs correspond to two films obtained from different polymer blend solutions with $\phi_m = 0.45$, indicating that the polymer blend morphology is very reproducible, even

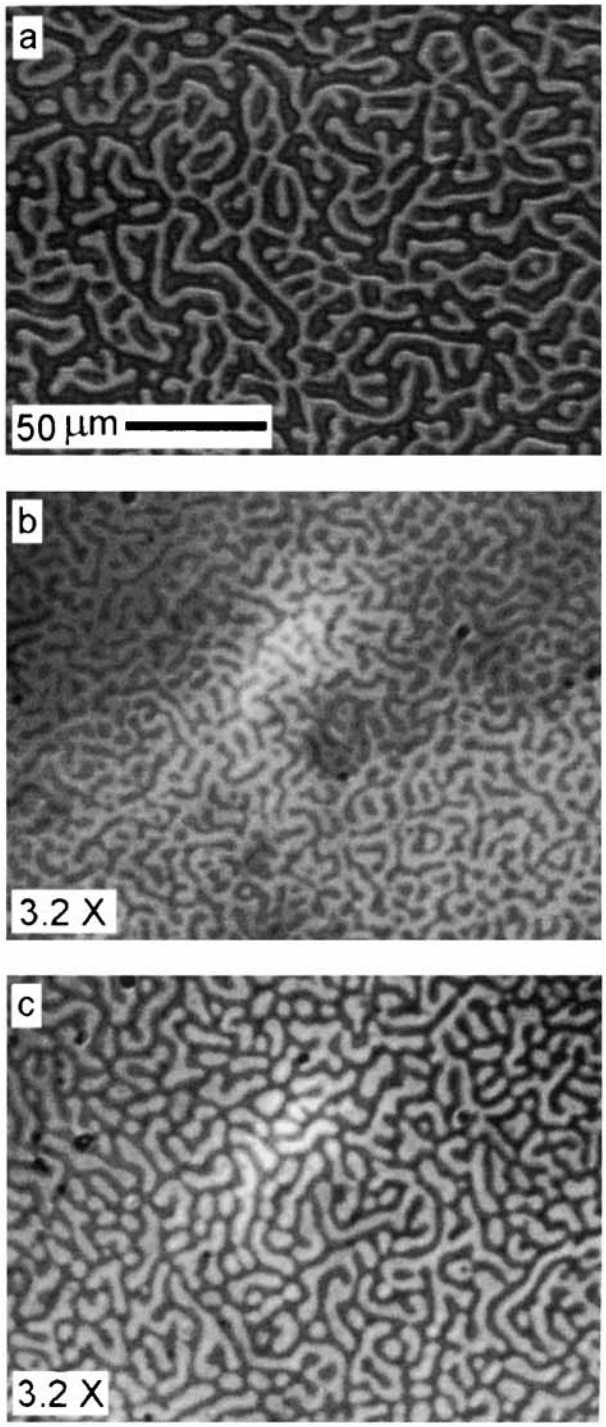

Figure 4. Morphology images for PS/PI blend films. (a) Si–SiO_x substrate, $h \sim 1000$ Å; (b) Si–SiO_x substrate, $h \sim 350$ Å; (c) Au/Pd substrate, $h \sim 350$ Å.

for ϕ_m values for which the morphology is very sensitive to changes in ϕ_m. The image quality is poor for the 350 Å thick films because there is very little optical contrast between the domains. The morphologies for the two substrates with the 350 Å thick films differ from the bicontinuous morphology observed for the 1000 Å thick films with the same value of $\phi_m = 0.45$. In addition, for the 350 Å thick films, there are significant differences between the morphologies observed for the two substrates. For the Si–SiO_x substrate, we observe PI-rich domains in a PS-rich matrix, and for the Au/Pd substrate, we observe PS-rich domains in a PI-rich matrix.

If we attribute the changes in morphology as the film thickness is decreased to a shift in $\phi_{m,b}$ due to the influence of the substrate, we can estimate this shift as follows. For the 350 Å thick film on Au/Pd the morphology observed for $\phi_m = 0.45$ is the same as that which is observed for the 1000 Å thick film for $\phi_m = 0.43$. Similarly, for the 350 Å thick film on Si–SiO_x the morphology observed for $\phi_m = 0.45$ is the same as that which is observed for the 1000 Å thick film for $\phi_m = 0.49$. This means that, as the film thickness is reduced, the value of $\phi_{m,b}$ shifts toward $\phi_{m,c} = 0.51$ for the Au/Pd substrate, and away from $\phi_{m,c}$ for the Si–SiO_x substrate. This result is in agreement with the observation that PS wets Au/Pd more readily than it does the Si–SiO_x surface. For the 350 Å thick films, we estimate a total shift of 0.06 in the $\phi_{m,b}$ values due to the difference between the Si–SiO_x and the Au/Pd substrates. We also measured the morphology for films of intermediate thicknesses (350 Å $< h <$ 1000 Å) on the Si–SiO_x and Au/Pd substrates, and we observed film thickness-related morphology shifts only for $h <$ 600 Å.

To evaluate the usefulness of the solvent quench experiment, it is helpful to compare it directly to the conventional temperature quench experiment. There are similarities between the two experiments, but also fundamental differences.

In the temperature quench experiment[10] for an upper critical solution temperature blend system, the binary polymer blend sample of a particular composition ϕ_m is prepared at a temperature T greater than that corresponding to the binodal temperature T_{bin} for that value of ϕ_m [see the schematic phase diagram shown in Fig. 5(a)]. The temperature is decreased quickly (during a short quench time t_Q) to the quench temperature T_Q, which lies within the metastable or unstable region of the phase diagram. The temperature is then held constant at T_Q as phase separation occurs during a time t at a single point (ϕ_m, T_Q) on the phase diagram. The quench time t_Q is usually negligible compared with the phase separation time t. The quench depth is controlled directly in the experiment by the choice of the quench temperature T_Q.

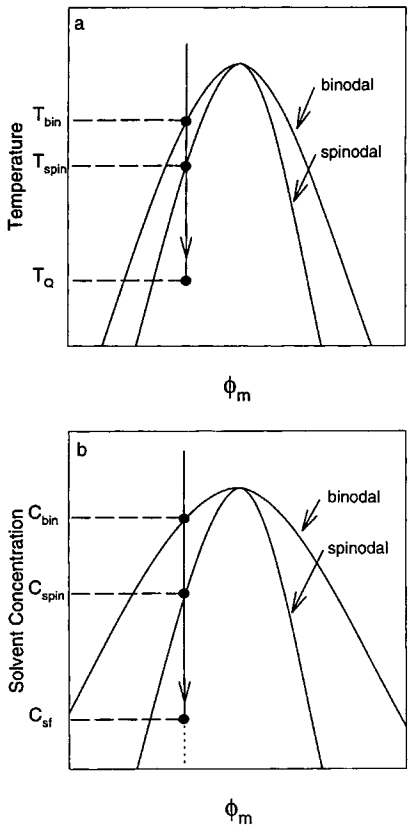

Figure 5. Schematic phase diagrams for (a) the temperature quench experiment, and (b) the solvent quench experiment. The symbols are explained in the text.

In the solvent quench experiment, the ternary blend solution (solvent plus binary polymer blend) is prepared with a particular relative mass fraction ϕ_m of the two polymers. The solution is dilute and therefore homogeneous (the solvent concentration C_s is only slightly less than 100%). The spincoating process leads to phase separation of the polymer blend as the solvent concentration C_s decreases rapidly due to evaporation of the solvent. We can understand the solvent quench experiment most easily by considering the phase diagram shown in Figure 5(b), in which we have plotted C_s as a function of ϕ_m. The phase separation process begins as C_s decreases below the concentration C_{bin} corresponding to the binodal line. Because the solvent quench is so rapid, phase separation effectively occurs only after C_s decreases below the concentration C_{spin} corresponding to the spinodal line. Also, there is a limiting value of C_s, C_{sf}, below which phase separation

stops because the molecules of one of the polymer species are no longer mobile. Therefore, for the solvent quench experiment, phase separation occurs at constant (room) temperature as C_s decreases rapidly from C_{spin} to C_{sf} during the short quench time t_Q. Unlike the temperature quench experiment, phase separation occurs not at a fixed point on the phase diagram but rather as the concentration decreases rapidly from C_{spin} to C_{sf}. Phase separation occurs as C_s decreases because the phase separation time t is usually comparable to the quench time t_Q for the solvent quench experiment. With $C_s < C_{sf}$, the phase separation morphology does not change with time if one of the polymers is glassy at room temperature. The quench depth, which for this experiment is the difference between C_{spin} and C_{sf}, is determined by the choice of solvent and polymers, as well as the spincoating conditions such as the spin speed. It is important to note that the quench depth in general varies with ϕ_m. For the simplest case in which C_{sf} is constant for all values of ϕ_m, the quench depth and quench time t_Q are largest for a critical quench and decrease for larger and smaller values of ϕ_m. The dependence of the quench parameters on ϕ_m is a fundamental characteristic of solvent quench experiments used to probe phase separation in thin films. Further theoretical work is required to extract all of the information from the experimental data.

As stated in the introduction, the solvent quench experiment is useful because it allows the study of polymer blends in which the two high molecular weight polymers have vastly different glass transition temperatures T_g. The measurement of the average domain area for different values of ϕ_m is useful because it forms a characteristic signature of the polymer blend system which can be studied as experimental parameters, e.g., final film thickness, are varied. Although comparisons of the average domain area for values of ϕ_m that are very different are complicated by the variation of the phase separation kinetics with ϕ_m, we can use the plots of average domain area versus ϕ_m to identify features for which the changes in the average domain area with ϕ_m are large. The most prominent feature in Figure 3 for the films on the Au/Pd and Si–SiO_x substrates corresponds to $\phi_m = \phi_{m,b}$, for which the bicontinuous morphology is observed. We can also identify an abrupt decrease in the average domain area as ϕ_m is increased above $\phi_m = 0.71 \pm 0.05$. We believe that this feature corresponds to the coincidence of C_{spin} with the limiting value of the concentration C_{sf}. For $\phi_m > 0.7$ there are very few, small phase-separated domains; these are likely formed by nucleation and growth.

SUMMARY AND CONCLUSIONS

The morphology of phase separation was studied as a function of the PS mass fraction ϕ_m in PS/PI blend thin films. Both polymer components were dissolved in a common solvent (toluene), and the polymer blend was quenched at room temperature by rapid evaporation of the solvent using spincoating. By systematically measuring the average area of the phase-separated domains as a function of ϕ_m, we have a sensitive probe of the effect of the substrate on the phase separation process. For 1000 Å thick films, we observe a large difference in the domain morphologies for Si–H and Si–SiO_x substrates due to the differences in the wetting properties of PS for the two surfaces. Little difference is observed between the morphologies for the Si–SiO_x and Au/Pd substrates for $h \sim 1000$ Å because the phase separation morphology is determined by the surface tensions of the polymers. For $h < 600$ Å, we observe small substrate-induced morphology shifts.

We thank Drs. R. C. Desai, B. G. Nickel, D. E. Sullivan, and J. M. Torkelson for helpful discussions. We also thank A. Smith for use of the sputtering system and image analysis software. The financial support of the Natural Sciences and Engineering Research Council (NSERC) of Canada is gratefully acknowledged.

REFERENCES AND NOTES

1. T. M. Rogers and R. C. Desai, *Phys. Rev. B*, **39,** 11956 (1989).
2. F. Bruder and R. Brenn, *Phys. Rev. Lett.*, **69,** 624 (1992).
3. M. Geoghegan, R. A. L. Jones, R. S. Payne, P. Sakellarion, A. S. Clough, and J. Penfold, *Polymer*, **35,** 2019 (1994).
4. S. Puri and K. Binder, *Phys. Rev. E*, **49,** 5359 (1994).
5. M. Geoghegan, R. A. L. Jones, and A. S. Clough, *J. Chem. Phys.*, **103,** 2719 (1995).
6. H. L. Frisch, P. Nielaba, and K. Binder, *Phys. Rev. E*, **52,** 2848 (1995).
7. C. K. Haas and J. M. Torkelson, *Phys. Rev. Lett.*, **75,** 3134 (1995).
8. H. Tanaka, *Phys. Rev. Lett.*, **76,** 787 (1996).
9. P. Keblinski, S. K. Kumar, A. Maritan, J. Koplik, and J. R. Banavar, *Phys. Rev. Lett.*, **76,** 1106 (1996).
10. J. D. Gunton, M. San Miguel, and P. S. Sahni, in *Phase Transitions and Critical Phenomena*, Vol. 8, C. Domb and J. L. Lebowitz, Eds., Academic Press, London, 1983.
11. J. W. Cahn, *J. Chem. Phys.*, **42,** 93 (1965).

12. A. Chakrabarti, *Phys. Rev. B,* **45,** 9620 (1989).
13. P. K. Chan and A. D. Rey, *Comput. Mater. Sci.,* **3,** 377 (1995).
14. H. Tanaka, T. Yokokawa, H. Abe, T. Hayashi, and T. Nishi, *Phys. Rev. Lett.,* **65,** 3136 (1990).
15. M. Okada, K. D. Kwak, T. Chiba, and T. Nose, *Macromolecules,* **26,** 6681 (1993).
16. J. Läuger, R. Lay, S. Maas, and W. Gronski, *Macromolecules,* **28,** 7010 (1995).
17. T. M. Slawecki, A. Karim, S. K. Kumar, T. P. Russell, S. K. Satija, C. C. Han, Y. Liu, M. H. Rafailovich, J. Sokolov, R. M. Overney, and S. A. Schwarz, to appear.
18. H. Tanaka, *Phys. Rev. Lett.,* **71,** 3158 (1993).
19. J. Läuger, C. Laubner and W. Gronski, *Phys. Rev. Lett.,* **95,** 75 (1995).
20. Polymer samples were obtained from Polymer Source Inc.
21. E. Yablonovitch, D. L. Allara, C. C. Chang, T. Gmitter, and T. B. Bright, *Phys. Rev. Lett.,* **57,** 249 (1986).
22. M. Niwano, J. Kageyama, K. Kurita, K. Kinashi, I. Takahashi, and N. Miyamoto, *J. Appl. Phys.,* **76,** 2157 (1995), and references therein.
23. P. J. Flory, *Principles of Polymer Chemistry,* Cornell University Press, Ithaca, 1953.
24. M. Kurata, *Thermodynamics of Polymer Solutions,* Harwood Academic Publishers, New York, 1982.

Received April 17, 1996
Revised July 22, 1996
Accepted July 24, 1996